

ASYMMETRIC DRIFT MAP OF THE MILKY WAY DISK POPULATIONS BETWEEN 8–16 KPC WITH LAMOST AND GAIA DATASETS

XIN LI¹, PENG YANG², HAI-FENG WANG^{1,3,4}, QING LI⁵, YANG-PING LUO¹, ZHI-QUAN LUO¹, AND GUAN-YU WANG¹

¹Department of Astronomy, China West Normal University, Nanchong, 637002, P. R. China

²Urban Vocational College of Sichuan, Chengdu, 610101, P. R. China

³CREF, Centro Ricerche Enrico Fermi, Via Panisperna 89A, I-00184, Roma, Italy

⁴Department of Physics, Sapienza, University of Rome, Piazzale Aldo Moro 5, I-00185 Rome, Italy and

⁵Jiangmen Experimental Middle School of Guangdong, Jiangmen, 529000, P. R. China

Version October 3, 2023

ABSTRACT

The asymmetric drift (AD) tomography in different populations will be helpful for us to better understand the disk kinematics, dynamics and rotation curves. Using the common stars from the LAMOST and Gaia surveys as well as circular velocity of Gaia DR3, we qualitatively explore the asymmetric drift distribution of the Galactic disk from 8–16 kpc. In the $R - Z$ plane, we find the asymmetric drift near the plane of the Galactic disk is small, and then gradually increases with the increase of the vertical distance, which makes the asymmetric drift appear as a “horn” shape in the $R - Z$ plane. Meanwhile, we reveal that high $[\alpha/\text{Fe}]$ populations have larger asymmetric drift than that in the low $[\alpha/\text{Fe}]$ populations. The asymmetric drift around the solar location $V_a = 6 \text{ km s}^{-1}$ and the asymmetric drift median value of the whole sample is 16 km s^{-1} . Moreover, we also find that the asymmetric drift median value in the north (20 km s^{-1}) of the Galactic disk is larger than that in the south (13 km s^{-1}), all errors are within 2 km s^{-1} . Furthermore, when we investigate the asymmetric drift of the Galactic disk in the mono-age stellar populations, we also find that the older stellar populations have larger asymmetric drift and velocity dispersion which is consistent with predictions of previous numerical models. Finally, based on the chemistry, we unveil that the average asymmetric drift of the thick disk is much higher than that of the thin disk.

Subject headings: Milky Way Galaxy; Milky Way disk;

1. INTRODUCTION

The Milky Way is the cornerstone for us to understand disk galaxies for the structure, formation and evolution. The Milky Way disk has a large portion of baryonic matter with the formation of stars as well as long-term evolution (van der Kruit & Freeman 2011). The six dimensional phase space distribution and dynamical properties, in turn, can be used to unveil some physical processes about the internal interactions and external disturbances of the Galactic disk and Galactoseismology ((Widrow et al. 2012, 2014; Carlin et al. 2013; Williams et al. 2013; Siebert et al. 2012; López-Corredoira et al. 2020; Wang et al. 2018a,b, 2019, 2020a,b,c, 2022a, 2023a,b; Khoperskov & Gerhard 2022; Li et al. 2023; Yang et al. 2023; Drimmel et al. 2022; Antoja et al. 2023) and reference therein). For example, Antoja et al. (2018) used stellar velocity distribution from Gaia DR2 data to reveal substructures such as arches, ridges, and snail shells in the solar neighborhood caused by the phase mixing. Many works show that these substructures might be originated from the internal perturbations caused by the outer Lindblad resonance of the Galactic bar and spiral arms dynamics (Kawata et al. 2018), stellar orbits captured by spiral resonance (Barros et al. 2020). The interaction between the Milky Way and the Sagittarius galaxy (Bin-

ney & Schönrich 2018; Khanna et al. 2019; Laporte et al. 2020), etc.

When studying the velocity distribution of stars in three dimensions, it is found that stars show a non-axisymmetric distribution in azimuthal velocity, which is described as asymmetric drift. We used to think of the motion of stars in the Galactic plane as a relatively simple circular or elliptical orbit. Due to the perturbations or non-equilibrium state of the disk, some stars deviate from the disk and move upward, causing angular momentum to decrease. Therefore, the phenomenon of asymmetric azimuthal velocity distribution is called asymmetric drift (Binney & Tremaine 2008). Or it can be defined as the difference between the velocity of stars with perfectly circular orbits in the Milky Way and the median tangential or azimuthal velocity of the population (Golubov et al. 2013).

Golubov et al. (2013) pointed out the problem between age and velocity dispersion for the V_a and V_\odot . The reason is that if the Jeans equation is applied to the stellar population with different ages, the velocity dispersion of the sample will increase gradually with the increase of age due to the age-velocity dispersion relations. The solution to the problem is to use some not-too-young stellar population whose median tangential velocity depends linearly on the square of the velocity dispersion, which can be extrapolated to a velocity dispersion equal to zero

to determine V_{\odot} .

Through this process, the Jeans equation takes the form of Eq. 4 (linear Strömberg equation) in [Golubov et al. \(2013\)](#), they redetermined the LSR based on standard assumptions of radial scale lengths independent of velocity dispersion in each metallicity bin and obtained a new solar peculiar motion. [Dehnen & Binney \(1998\)](#) also measured the velocity of the Sun relative to the LSR in the direction of Galactic rotation and found that the asymmetric drift linearly depends on the square of the total velocity dispersion of the stellar population. Using Hipparcos data, [Aumer & Binney \(2009\)](#) also used the same method to obtain a velocity with a small error of V_{\odot} . Different methods and models seem to affect the calculation of the peculiar motion of the Sun ([Binney 2010](#)) and the modelling progress about asymmetric drift around the Sun can also be found in [Binney et al. \(2014\)](#). The local rotation curve (RC) and asymmetric drift were detailed discussed and analysed using RAVE and SEGUE sample in [Sysoliatina et al. \(2018\)](#). Recently, we are also considering the asymmetric drift effect in the rotation curve in more details ([Jiao et al. 2023](#)) with the Jeans equation.

[Williams et al. \(2013\)](#) found that the asymmetric drift varies with vertical height can be 40 km s^{-1} between the midplane and $Z = 2 \text{ kpc}$. [Robin et al. \(2017\)](#) investigated disk kinematics using Gaia DR1 and Radial Velocity Measurement Experiments (RAVE4) high latitude sample ([Kordopatis et al. 2013](#); [Steinmetz et al. 2020a,b](#)). In addition, they also studied the asymmetric drift of the Galactic disk by fitting stackel potential to orbit. Using the above method, [Robin et al. \(2017\)](#) studied the asymmetric drift of thin disk and thick disk (young and old) at different ages as a function of Galactocentric distance and vertical distance based on the mock data. In the R_{lag} - V_{lag} (asymmetric drift) diagram, they found that the asymmetric drift is inclined to decrease as the Galactocentric distance increases. In the Z_{lag} - V_{lag} diagram, the asymmetric drift gradually increases with the increase of vertical distance.

The contribution of asymmetric drift is not only in the stellar velocity profile of the Milky Way but also the rotation curve of the Milky Way. However, so far, we have poor understanding about exploring the asymmetric drift distribution of the Galactic disk in different age and abundance populations beyond solar neighborhood, to the best of our knowledge. The aim of this paper is using the LAMOST DR4 and Gaia DR3 data as well as a basic dynamic formula, to quantify the asymmetric drift of mono-age-abundance populations of stars in the Galactic disk and provide the purely observational asymmetric drift maps, which will be quite useful for us to discuss the topics of the disk asymmetries and rotation curves in the future, at least from the statistical and qualitative point of view. At this stage we do not use the Jeans analysis like previous works but make full use of the abundant phase space properties in different populations under the assumption of the disk rotation curve, and the rotation curve patterns in different populations will be shown in the next step.

The paper is structured as follows: In Section 2, we describe the chemical abundance, age information and three-dimensional velocity of the sample, as well as the

model or formula we used to calculate asymmetric drift; In Section 3 we present our main results for the AD maps in the different space; In Section 4, we discuss the results of asymmetric drift, and in Section 5, we summarize the results of this paper.

2. DATA AND METHODS

2.1. Sample

Guo Shoujing telescope, Large Sky Area Multi-Objective Fiber Optic Spectroscopic Telescope (LAMOST) is a new type of telescope with large field of view and large aperture, namely “reflective Schmidt telescope”, with an effective aperture of 4 m. Its controllable fiber positioning technology enables it to place 4,000 optical fibers in a focal plane of 1.75 meters in diameter with a field of view of five degrees, obtaining spectral coverage of 370 nm – 900 nm ([Zhao et al. 2012](#); [Deng et al. 2012](#)).

The stellar parameters of our sample comes from the red giant branch stars (RGB) of LAMOST DR4 selected by [Wu et al. \(2019\)](#). The age and its error were determined by the kernel principal component analysis method (KPCA) with an uncertainty of 30%. The uncertainty of the radial velocity is 5 km s^{-1} , which is obtained using the LAMOST stellar parameter pipeline of Peking University (LSP3). When using LSP3 to determine stellar parameters, the accuracy of effective temperature can reach 100 K, the accuracy of surface gravity can reach 0.1 dex, respectively ([Xiang et al. 2017](#)). The metallicity and elemental abundances of stars are obtained by cross-matching with the stellar catalogue derived by [Xiang et al. \(2019\)](#) using the data-driven Payne method. [Xiang et al. \(2019\)](#) used the data-driven Payne (DD-Payne ([Ting et al. 2019](#))) modelling method to determine the parameters and element abundances of 6 million stars from the 8 million low resolution ($R=1800$) spectra of LAMOST DR5. The error of metallicity is 0.1 dex, and the error of $[\alpha/\text{Fe}]$ is about 0.05 dex. The distance in the catalog is estimated by the Bayesian estimation method ([Carlin et al. 2015](#)) calibrated by [Xu et al. \(2020\)](#), which is about 15% uncertainty.

The proper motion in this paper is from the Gaia DR3 dataset that we cross-matched and we do not set the cut on the renormalized unit weight error (RUWE) in order to keep the enough sampling, and which might increase the dispersion but will not change our final conclusions. This database contains the position of stars, proper motion, parallax and other parameter information. The proper motion and parallax of Gaia DR3 achieve high accuracy ([Gaia Collaboration et al. 2022](#)), more details can also be found in [Yang et al. \(2023\)](#).

2.2. Velocity coordinates

The kinematic and coordinate distribution of these RGB stars are obtained through the coordinate transformation in Galpy ([Bovy 2015](#)). For some parameters of coordinate transformation, the distance from the position of the Sun to the center of the Milky Way is 8.34 kpc ([Reid et al. 2014](#)), and the vertical distance from its position to the Galactic disk is 27 pc ([Chen et al. 2001](#)). For the local standard of rest, we use the 238 km s^{-1} calculated by [Schönrich \(2012\)](#). The Solar peculiar motion relative to LSR are (9.58, 10.5, 7.01) km s^{-1} , respec-

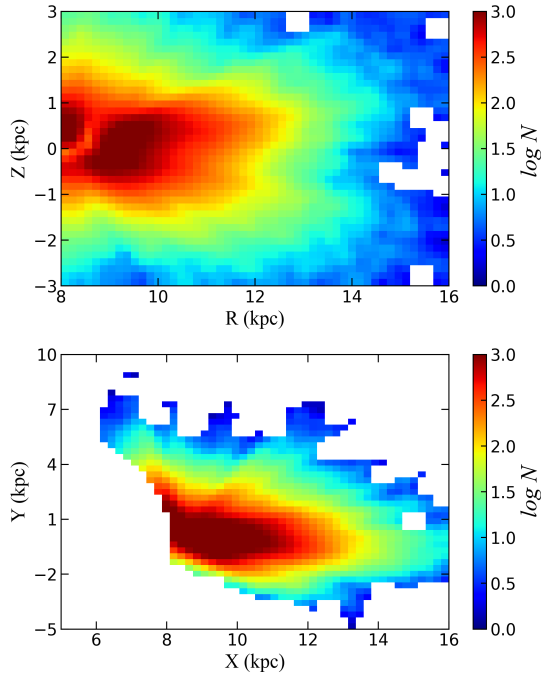


FIG. 1.— Top panel: The smoothed distribution of RGB stars in the $R - Z$ plane used in this work, the number of stars coloured in log scale in the north of the Galactic disk is more than that in the south of the Galactic disk for this sample. Bottom panel: the distribution of RGB stars in the $X - Y$ plane. The bin size is 0.16 kpc for R , 0.15 kpc for Z ; 0.22 kpc for X , 0.32 kpc for Y .

tively (Tian et al. 2015). Combining these parameters, we can obtain six dimensional properties for 300, 433 RGB stars. Note different solar motions will not change our final conclusions in this work. We have adopted a Galactocentric cartesian coordinates with X increasing outward from the Galactic centre, Y in the direction of rotation, and Z positive towards the North Galactic Pole (NGP). Cylindrical velocities V_R , V_ϕ , and V_Z are defined as positive with increasing R , ϕ , and Z .

We make some constraints as follows in order to mainly focus on the disk region:

- (1) $8 < R < 16$ kpc and $-3 < Z < 3$ kpc (we focus on the outer thin and thick disk region);
- (2) $0 < \text{Age} < 14$ Gyr (removing some stars older than 14 Gyr, which is not true);
- (3) $[\text{Fe}/\text{H}] > -1.5$ and $[\alpha/\text{Fe}] < 0.35$;
- (4) $-150 < V_R < 150$ km s $^{-1}$, $-50 < V_\phi < 350$ km s $^{-1}$ and $-150 < V_Z < 150$ km s $^{-1}$;

Using these constraints, we finally get 231, 874 RGB stars. Figure 1 shows the spatial distribution of our stellar sample in the $R - Z$ and $X - Y$ cylindrical and Cartesian coordinate planes, respectively, coloured by the number of stars on the logarithmic scale. From the density distribution of stars, we can see that there are more stars on the northern side of the disk than on the southern side for our sample and the disk flaring features can be found on the top panel.

2.3. Method for Asymmetric drift

In order to calculate the asymmetric drift, we adopt the method mentioned by Golubov et al. (2013), which can be found more details in Binney & Tremaine (2008) (Sec. 4) and the equation is as follows:

$$V_a = \bar{V}_{c(R)} - \bar{V}_\phi(R) = \Delta V - V_\odot \quad (1)$$

$$V_{c(R)} = 229 - 2.3(R - R_\odot) \quad (2)$$

Where R represents the distance from the Galactic center, the distance between the Sun and the Galactic center is 8.34 kpc, $\bar{V}_c(R)$ represents the median rotational velocity, and $\bar{V}_\phi(R)$ represents the median azimuth velocity in the volume. Then the first calculation method of V_a can be expressed as the mean (median) rotational velocity minus the mean azimuthal velocity. The latter formula of which is expressed as the median tangential velocity minus the peculiar motion of the Sun which is suitable for the local volume. Eq. (2) shows how the rotational velocity is calculated. In this paper we fully calculate the asymmetric drift using the mean rotational velocity minus the mean azimuth velocity. The circular velocity value around the Sun and the slope are adopted from Eilers et al. (2019) and Wang et al. (2023a), both works of rotation curves are consistent for the overall trend with different solar motions, LSR values and stellar tracers. As mentioned, we focus on the statistical law and pattern in different populations, and RC populations which is not so simple will be shown in the future work, more information also can be found in the conclusion part.

3. RESULTS

3.1. Asymmetric Drift Distribution for the Entire Sample

We calculate the asymmetric drift of the entire sample and map the distribution of the asymmetric drift of the Galactic disk using the equation mentioned by Golubov et al. (2013). Figure 2 shows the distribution of velocity and asymmetric drift of the sample in chemical space ($[\text{Fe}/\text{H}]$ - $[\alpha/\text{Fe}]$). The first three panels show the velocity distribution of stars in the cylindrical coordinates of the Galactic center, the 3D motions on the chemical plane, as seen, there is no clear trend for the radial velocity and vertical velocity distribution, but for the azimuthal velocity, the higher for the $[\alpha/\text{Fe}]$, the lower for the velocity value, it might imply the halo and disk populations properties. Especially for the bottom right one shows the distribution of asymmetric drift. The velocities of stars in the Galactic coordinates show clear patterns for thin disk with $[\alpha/\text{Fe}]$ around 0.0 dex and thick disk with $[\alpha/\text{Fe}]$ around 0.2 dex, for example the thin disk is rotating faster than the thick disk. For the asymmetric drift diagram at the bottom, it shows that the thin disk population is within 10 km s $^{-1}$ but the thick disk is much larger, can be larger than 40 km s $^{-1}$, we must admit it depends on the solar motions and LSR and model assumption, in this work, as mentioned above, we just want to investigate the statistical law of asymmetric drift in different populations.

The upper panel of Figure 3 shows the distribution of asymmetric drift in the $R - Z$ plane and $X - Y$ plane, the value is from 0 to 60 km s $^{-1}$ on the left panel and 0 to 50 km s $^{-1}$ on the top right panel, while the lower panel of Figure 3 shows the error distribution by bootstrap. The error is mainly contributed by the distance uncertainty, proper motion uncertainty, radial velocity.

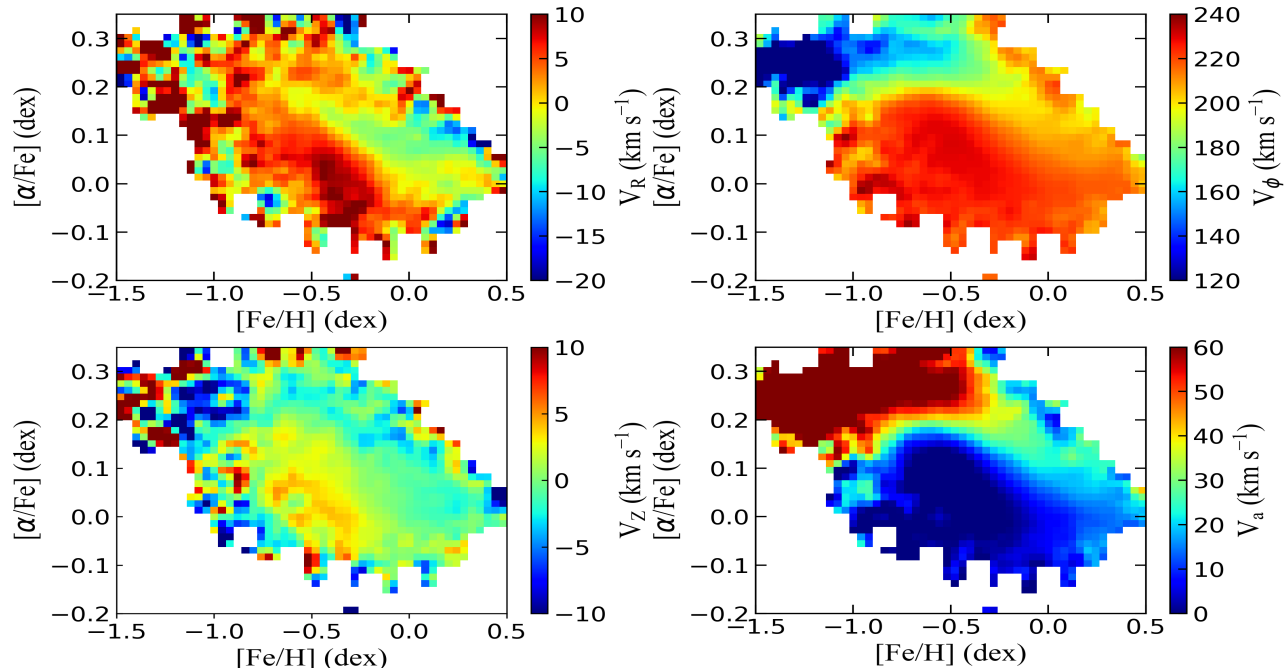


FIG. 2.— Top panel: the stars Galactic radial (V_R), azimuthal (V_ϕ) on the $[\text{Fe}/\text{H}]$ and $[\alpha/\text{Fe}]$ plane. Bottom panel: the stars Galactic radial (V_Z) and asymmetric drift (V_a) velocities on the $[\text{Fe}/\text{H}]$ and $[\alpha/\text{Fe}]$ planes. The bin size is 0.04 dex for $[\alpha/\text{Fe}]$ and 0.01 dex for $[\text{Fe}/\text{H}]$.

Bootstrap errors are determined by resampling (with replacement) 100 times for each bin, and the uncertainties of the estimates are determined using 15 per cent and 85 per cent percentiles of the bootstrap samples. For both components, most of the bootstrap errors are less than 2 km s^{-1} for the AD errors. Using the Eq. (2) of asymmetric drift, we find that the median value of asymmetric drift of the whole sample is $V_a = 16 \text{ km s}^{-1}$ in the $R-Z$ plane. When we have a careful analysis for the distribution of asymmetric drift in the $R-Z$ plane, we find that the asymmetric drift near the plane of the Galactic disk is smaller for the overall trend, and the asymmetric drift gradually increases with the increase of vertical distance. With the increase of Galactocentric distance and vertical distance, the change of asymmetric drift in the northern part of the disk is also clearer than that in the southern part. This change along with the Galactocentric and vertical distance makes the asymmetric drift like a “horn” in the $R-Z$ plane, which is almost consistent with the result of Katz. (2018). As shown in Figure 4, when we investigate the distribution of asymmetric drift in the north and south sides of the disk, the asymmetric drift is increasing with the vertical distance and decreasing with the radial distance. When calculating the median value of the average asymmetric drift of the northern and southern sides of the disk, we find that the median of the asymmetric drift of the northern side (20 km s^{-1}) is relatively larger than that of the southern side (13 km s^{-1}) with errors within 2 km s^{-1} , which in turn proves that the “horn” bends downward with the increase of the Galactocentric distance, but we must admit this is based on the assumption, which might not be so significant for this statistical patterns analysis.

The upper right panel of Figure 3 shows the distribution of the asymmetric drift in Cartesian coordinates.

Compared with the distribution of asymmetric drift in cylindrical coordinates, the distribution in cartesian coordinates has no clear patterns, but it is showing the asymmetric drift is small around $Y=0$.

Moreover, we also present the asymmetric drift in the Galactic longitude and latitude plane as shown in Figure 5, the pattern is similar to the $R-Z$ plane, that is, the asymmetric drift near the low Galactic latitude is smaller, and the asymmetric drift at the high Galactic latitude is larger.

3.2. Asymmetric drift distribution of different age stellar populations

In this section, we explore the asymmetric drift distribution of stellar populations in different ages, namely, $[0, 2]$, $[2, 4]$, $[4, 6]$, $[6, 8]$, $[8, 10]$, $[10, 14]$ Gyr, a total of six different age populations.

Figure 6 shows the distribution of asymmetric drift in the $R-Z$ plane for stellar population of different ages. As seen in Figure 6, the asymmetric drift of stars younger than 6 Gyr is relatively smaller, and when the population is older than 6 Gyr, it shows the larger asymmetric drift, in particular far away from the disk. With the increase of age, the asymmetric drift on both sides of the disk increases very clearly. Older stars far away from the disk have a larger asymmetric drift than younger stars near the disk, which is not surprised, but as far as we know, beyond Solar neighborhood, almost all previous works have no age information to see the temporal evolution for the asymmetric drift kinematics.

Similarly, Figure 7 shows the distribution of asymmetric drift in the $X-Y$ plane for stellar population of different ages. We can clearly see that stars younger than 6 Gyr have relatively smaller asymmetric drift, and older stars still have much larger asymmetric drift. In

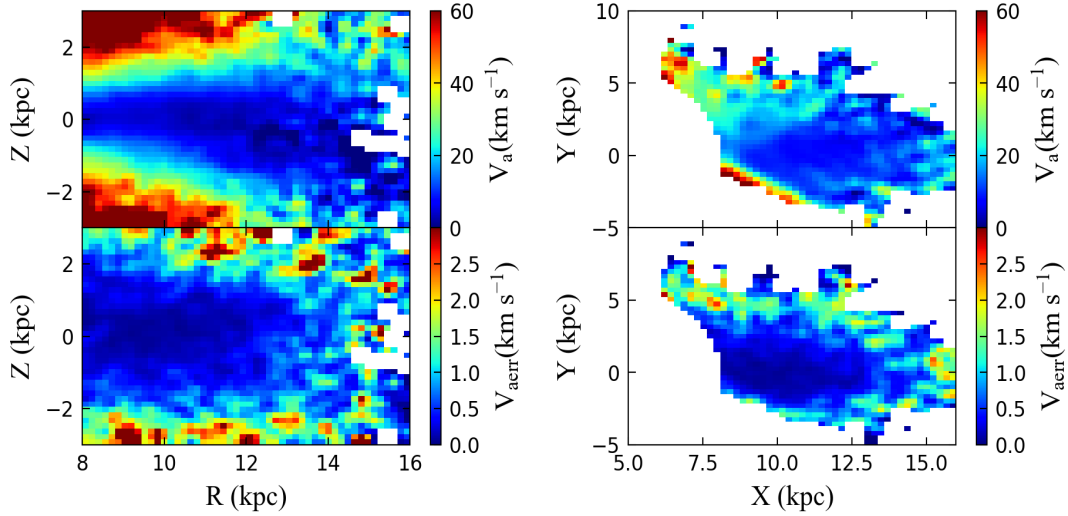


FIG. 3.— The asymmetric drift distribution of the final sample. The top diagrams show the distribution of asymmetric drift in the $R-Z$ and $X-Y$ planes, while the bottom diagrams show the corresponding error given by Bootstrap.

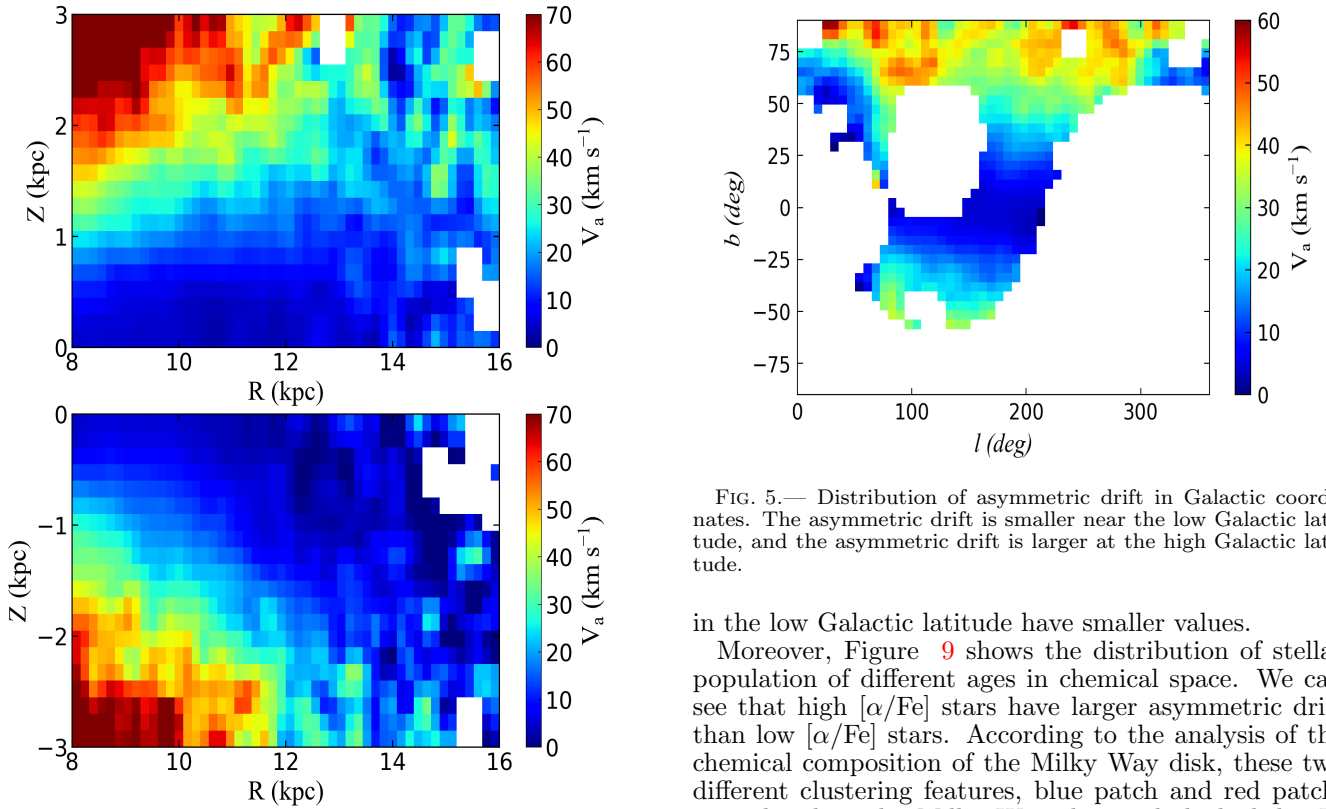


FIG. 4.— Top panel: asymmetric drift distribution of RGB stars in the north of the disk; Bottom panel: asymmetric drift distribution of RGB stars in the south of the disk. The asymmetric drift changes more sharply in the north than in the south.

the meantime, Figure 8 shows the distribution of asymmetric drift values of stellar population of different ages in Galactic coordinates. In sky coordinates, as can be seen, stars with age less than 6 Gyr show smaller asymmetric drift in the whole spatial distribution, but stars with age older than 6 Gyr located in the high Galactic latitude have larger asymmetric drift, in contrary, stars

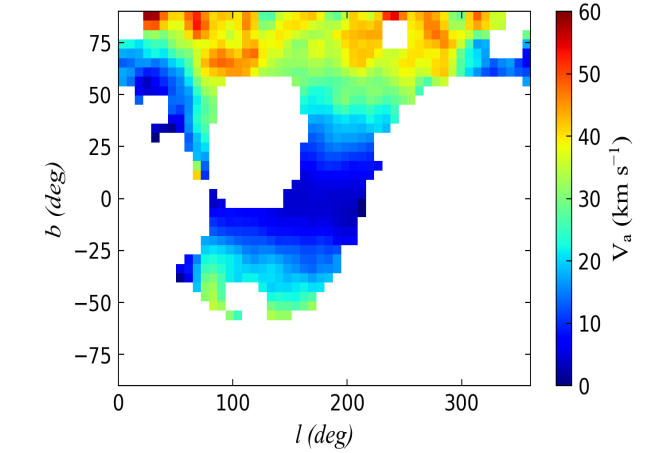


FIG. 5.— Distribution of asymmetric drift in Galactic coordinates. The asymmetric drift is smaller near the low Galactic latitude, and the asymmetric drift is larger at the high Galactic latitude.

in the low Galactic latitude have smaller values.

Moreover, Figure 9 shows the distribution of stellar population of different ages in chemical space. We can see that high $[\alpha/\text{Fe}]$ stars have larger asymmetric drift than low $[\alpha/\text{Fe}]$ stars. According to the analysis of the chemical composition of the Milky Way disk, these two different clustering features, blue patch and red patch, are related to the Milky Way thin and thick disk. In addition, we also find that stars of with $[\alpha/\text{Fe}] < -0.1$ dex tend to have larger asymmetric drift.

Finally, 1D variation of asymmetric drift with Galactocentric distance and vertical distance using stellar populations of different ages is shown in Figure 10. The black dotted dashed line represents the whole sample, and the dotted lines in other colours represent the samples of stellar population of different ages. We can see that when the Galactocentric distance is less than 16 kpc we investigated during this work, the asymmetric drift of the whole sample and different age populations show a relatively flat trend but with a slightly decreasing trend,

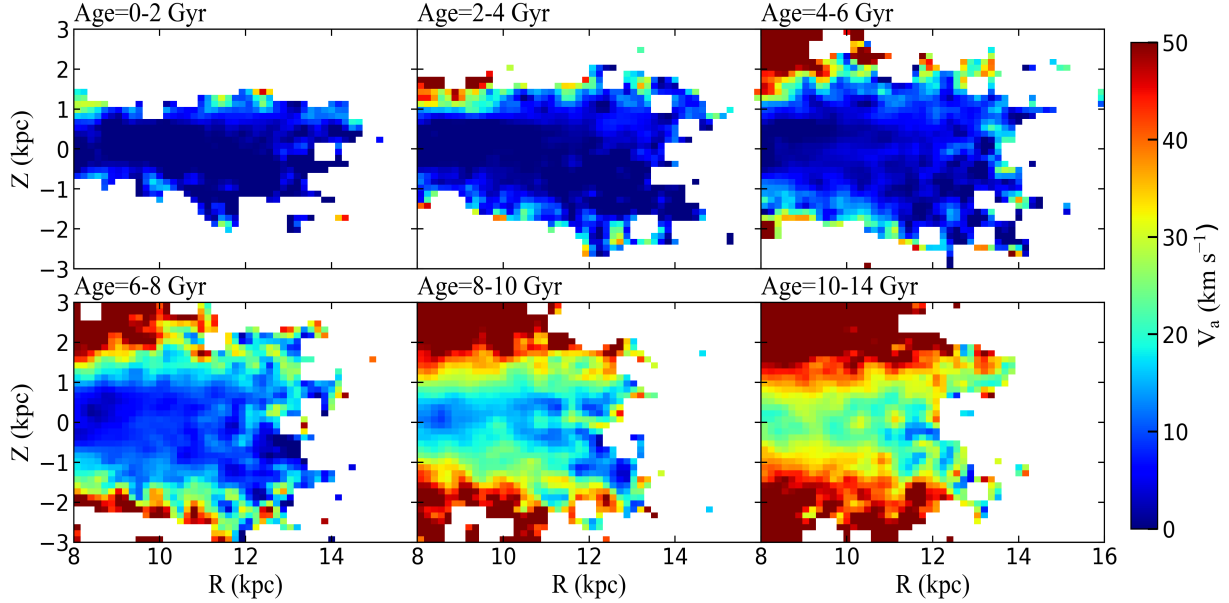


FIG. 6.— Distribution of asymmetric drift in the $R - Z$ plane for different age populations.

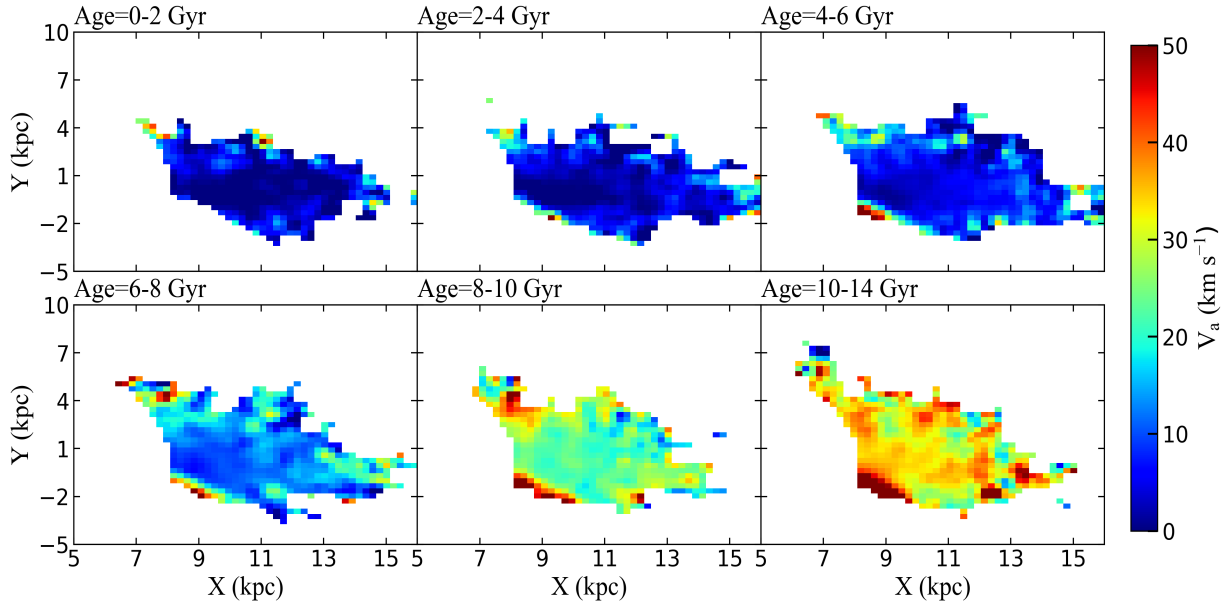


FIG. 7.— Distribution of asymmetric drift in the $X - Y$ plane for different age populations.

which is almost consistent with the modelling results of Robin et al. (2017) within 12 kpc based on mock data to compare Gaia DR1, although they only use high latitude stars with $[\text{Fe}/\text{H}]$ to separate thin and thick disk. For some regions like 13 kpc, the asymmetric drift curve has risen and fluctuated, which we think may be caused by the not homogenous sampling. For the vertical distance diagram, the asymmetric drift curve shows an “U” shape, that is, the asymmetric drift is larger at higher height, and smaller near the Galactic disk. The shape of the asymmetric drift curve is consistent with the previous results (Golubov et al. 2013) that the asymmetric drift near the galactic disk plane is small, while the asymmetric drift far away from the Galactic disk plane is relatively larger.

3.3. Asymmetric Drift Distribution of Thin and Thick disk

In this section, our main objective is to study the asymmetric drift distribution of thin and thick disk in the Milky Way galaxy. Figure 11 shows the density distribution of our sample in the metallicity and chemical abundance plane ($[\text{Fe}/\text{H}]$ - $[\alpha/\text{Fe}]$) which is used for us to divide the whole sample into two populations: thin and thick disk. In Figure 11, thick disk is shown above the upper dotted line, and thin disk sample is shown below the lower dotted line.

Similarly, Figure 12 shows the distribution of asymmetric drift in the $R - Z$ plane (left), $X - Y$ plane (middle) and Galactic coordinates (right) using the thin or thick disk sample (upper panel is thin disk, lower panel

is thick disk). Compared to the thin disk, the thick disk has the larger asymmetric drift in spatial distribution. The asymmetric drift of thin and thick disk increases with the increase of vertical distance, but the variation of asymmetric drift of thin disk with the increase of vertical distance is much weaker than that of thick disk. When we divide these two parts of data into the north and south sides of the disk again, as shown in Figure 13, the asymmetric drift of the thin (left panel) and thick disk (right panel) is clearly varying with the vertical distance. It is also found that the median value of asymmetric drift of thick disk (45 km s^{-1}) is much higher than that of thin disk (6 km s^{-1}) within few km s^{-1} uncertainties, it can be pointed that that we only care about the qualitative pattern so the error here is not so important, since we all know we are confirming the basic knowledge of the disk but with more population analysis.

Finally, as shown in Figure 14, the asymmetric drift curve (top two panels comparison) of the thin and thick disk shows a relatively flat trend within 14 kpc, and beyond that, the number of sample decreases and the data sampling is insufficient enough, leading to fluctuations, and the asymmetric drift curve along with the vertical height of the thin disk is clearly flatter and smaller. In the vertical distance panel of the thick disk, the asymmetric drift curve also roughly presents an “U” shape. Compared to the asymmetric drift curve of the thick disk, the asymmetric drift curve of the thin disk is much flatter (bottom two panels), but it also has similar trend.

4. DISCUSSION

4.1. Comparison with other works

Motivated by the migration physics of the disk, Hayden et al. (2018) revealed the distribution of asymmetric drift when they used the Gaia-ESO survey data to study the orbital properties of metal-rich stars in the solar neighborhood and the kinematic properties of stellar populations. In addition, they found that most of the $[\text{Mg}/\text{Fe}]$ -rich stars have significant asymmetric drift with 40 km s^{-1} slower than the lower $[\text{Mg}/\text{Fe}]$ populations. The correlation between asymmetric drift and chemical elements can also be found in the current work, that is, stars with high $[\alpha/\text{Fe}]$ have larger asymmetric drift than stars with low $[\alpha/\text{Fe}]$. Compared to Gaia-ESO work, It is clear that we investigate the distribution of asymmetric drift mainly in the north side farther outer disk with age and $[\alpha/\text{Fe}]$. By analyzing the relations between the median rotational velocity and the square of the radial velocity dispersion for three different metal-rich populations, Golubov et al. (2013) found that metal-poor stars have smaller asymmetric drifts and larger rotational velocities, which is confirmed in this work (See Figure 2). We not only investigate the distribution of asymmetric drift in chemical space, but also reveal the distribution of different age populations fully beyond the solar location.

Sysoliatina et al. (2018) also presented analysis for the definition of asymmetric drift, that is, the lag of the tangential velocity of the stellar population with respect to the rotational curve. They obtained a new version of the Strömberg relation and a generalized version of the asymmetric drift expression by iterative calculation starting from the Jeans equation for a stationary and axisymmetric system. They also revealed that the asymmetric

drift diagram in stellar metallicity consistent with Golubov et al. (2013), that is, the asymmetric drift of metal-poor stars is smaller. Moreover, they found a gradient value of $0.98 \pm 1 \text{ km s}^{-1} \text{ kpc}^{-1}$ for the rotational velocity by considering the asymmetric drift correction for a range of Galactocentric distances from 7 to 10 kpc. We are currently extending the map in spatial and chemical space for the purely observational AD map analysis, it is clear that we know purely Gaia dataset can cover this range but so far we do not notice the full AD maps in populations until 16 kpc. Furthermore, Golubov et al. (2013) pointed out that the lower the metallicity, the larger velocity dispersion and larger radial scale-length, as well as smaller asymmetric drift and faster mean rotation, here we also present the analysis for the asymmetric drift along with the velocity dispersion and its distribution on the $[\text{Fe}/\text{H}]$ and $[\alpha/\text{Fe}]$ plane (see (See Figure 15) and Figure 16). As can be seen, the asymmetric drift increases with the increasing dispersion, and the older the stars, the larger for the overall trend. Meanwhile, the dispersion value, which is implying the dynamically cold or hot for the population, shows that the thick disk population (high $[\alpha/\text{Fe}]$) is hotter than the thin disk population (low $[\alpha/\text{Fe}]$), generally, the younger the population (top three panels), the colder the dynamics, vice versa (bottom three). Using Gaia DR3 and RAVE DR5 data to study the kinematic properties of the thin and thick disk of the Milky Way in the solar neighborhood, Vieira et al. (2022) found that the median rotational velocities of the thin and thick disk lag the assumed velocities of the local standard of rest. The thin disk lags the local stationary rotation velocity by $5 \sim 8 \text{ km s}^{-1}$, and the median rotation velocity of the thick disk in the solar neighborhood lags the rotation velocity of the LSR by 20 km s^{-1} . The reason for this phenomenon is caused by asymmetric drift. And Vieira et al. (2022) also pointed out that there are two reasons for this asymmetric drift phenomenon: one is the difference between the gravitational and centrifugal force caused by the non-zero component of the velocity dispersion of the system; the other is the mixing of thin and thick disk. During this work, we also find that the asymmetric drift of thick disk is significantly larger than that of thin disk with more populations details. In short, our current results confirm some progress for the overall trend and key arguments but in more other details and farther distance from the purely observational point of view (Pasetto et al. 2012; Guiglion et al. 2015; Wojno et al. 2023b; Robin et al. 2017).

Some modelling works of Milky-Way-like galaxies predict a systematic variation of the asymmetric drift with age and metallicity (Schönrich et al. 2010; Loebman et al. 2011). In Lee et al. (2011b) results, which were shown for the SEGUE G dwarf sample that the asymmetric drift in the thin disk decreases with decreasing metallicity in contrast to the naive expectation of local evolution models. From the qualitative view of point, we are confirming these observational and simulation results, but we have larger coverage or more population information during this work promoting us to understand better about disk kinematics and dynamics in the outskirts.

4.2. Different rotation curves comparisons

Eilers et al. (2019), Mróz et al. (2019) and Wang et al. (2023a) revealed the rotation curve gradient as -1.7 km

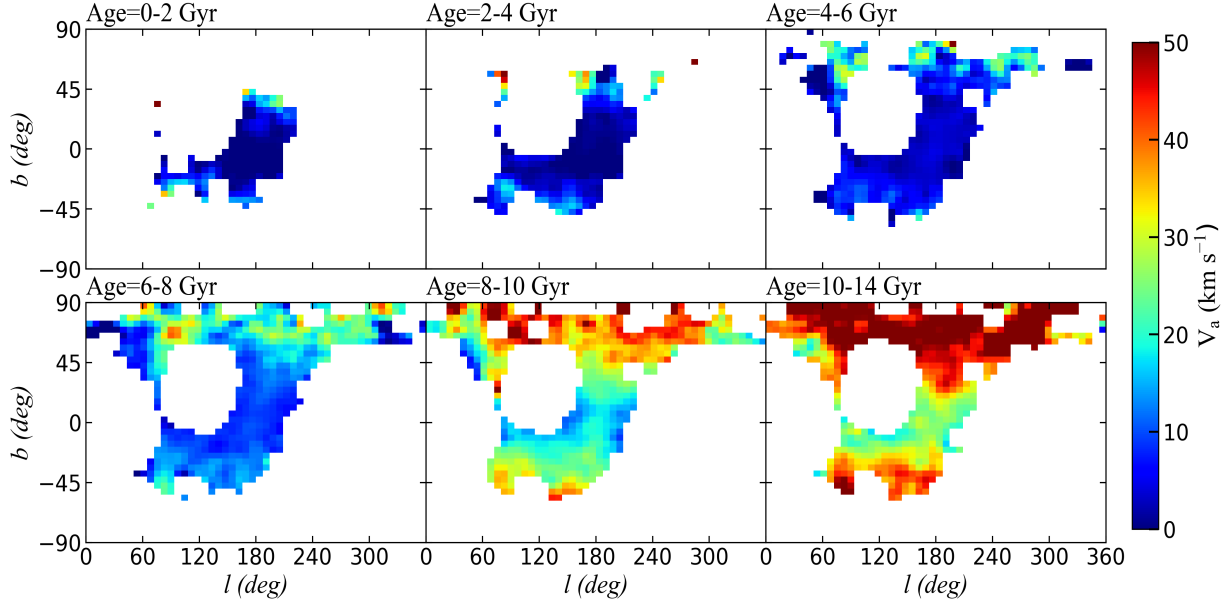


FIG. 8.— Distribution of asymmetric drift of different age stellar populations in sky coordinates.

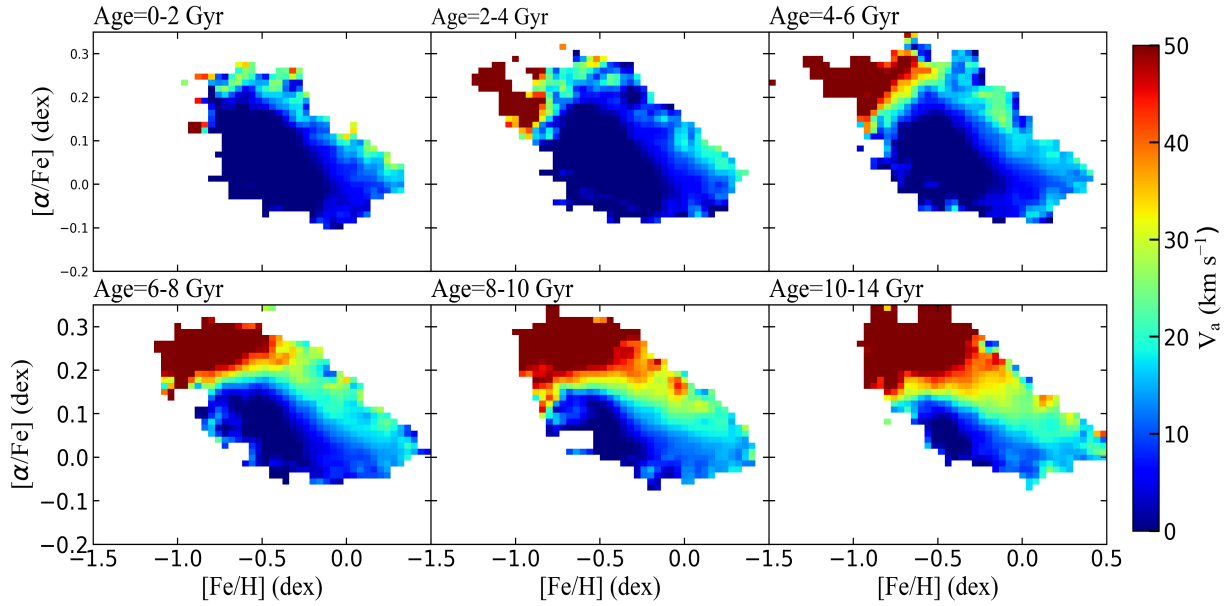


FIG. 9.— Distribution of asymmetric drift in the $[\text{Fe}/\text{H}]$ and $[\alpha/\text{Fe}]$ plane for different age populations.

$\text{s}^{-1} \text{ kpc}^{-1}$, $-1.41 \text{ kms}^{-1} \text{ kpc}^{-1}$ and $-2.3 \text{ kms}^{-1} \text{ kpc}^{-1}$, respectively. These are almost consistent within the range of this work with slightly different slopes. For the solar radius, motions and the LSR, different groups have adopted different values (Bland-Hawthorn & Gerhard 2016; Khoperskov & Gerhard 2022; Schönrich 2012). Figure 17 randomly shows the distribution of asymmetric drift in the $R-Z$ plane and $X-Y$ plane according to different rotation curve models, solar location and motions as well as LSR for more tests. We could find different circular velocity models and solar motions have influences on the asymmetric drift patterns and values, but for the overall trend, they are similar qualitatively, the systematics is clearly mainly caused by the different circular velocity at the sun. Again, we focus on the statistical

law of the asymmetric drift in different populations beyond Solar neighborhood.

5. CONCLUSIONS

In this paper, we crossed matched the LAMOST DR4 RGB stars with age and abundance and Gaia DR3 proper motion data to study the asymmetric drift distributions of the Galactic outer disk in different populations. Through calculation and analysis, the median value of asymmetric drift of the whole sample in the range ($R = [8, 16]$, $Z = [-3, 3 \text{ kpc}]$) is 16 km s^{-1} , and the value of asymmetric drift around the Sun is 6 km s^{-1} . By analysing the asymmetric drift distribution of the sample in the $R-Z$ plane, we find that the distributions of the asymmetric drift in the $R-Z$ plane present a

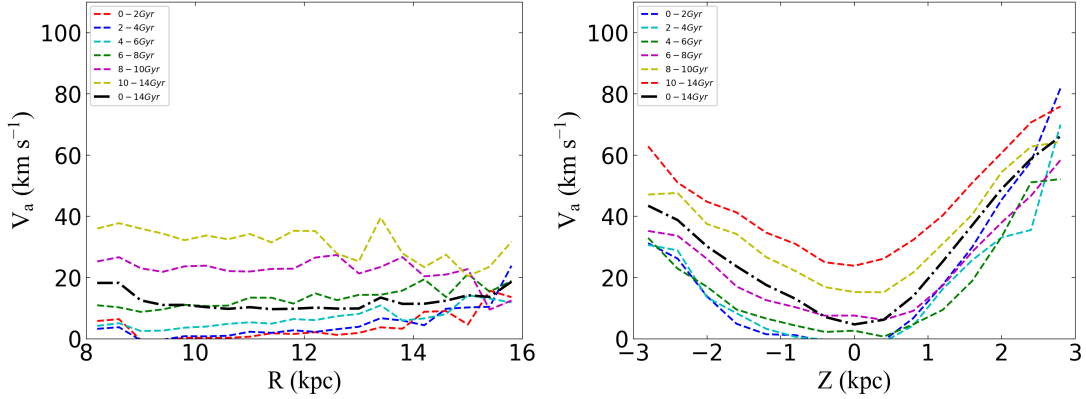


FIG. 10.— One-dimensional distribution of asymmetric drift in Galactocentric distance (R) and vertical distance (Z). The black bold dotted line represents the entire sample, and other dashed lines of different colours represent stellar population of different ages.

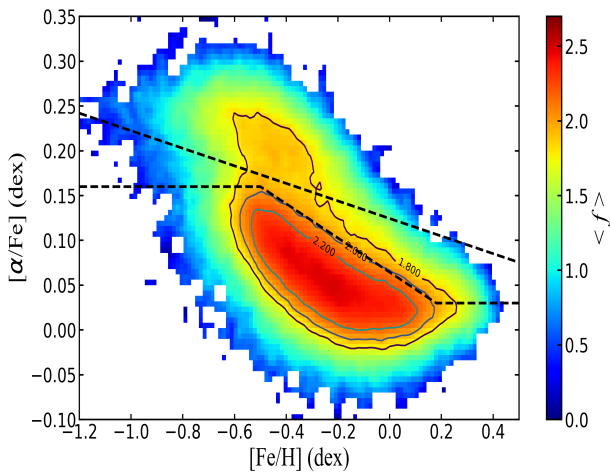


FIG. 11.— Density distribution, colored by the star counts in the log scale, of the sample in the $[\text{Fe}/\text{H}]$ and $[\alpha/\text{Fe}]$ plane. Two dashed lines used to separate the thin and thick disk stars.

“horn” shape, that is, as the Galactocentric distance increases, the asymmetric drift varies, the median asymmetric drift on the north side of the Galactic disk (20 km s^{-1}) is larger than the median value on the south side (13 km s^{-1}). In addition, we also find that the asymmetric drift showing an increasing trend with the increase of vertical distance clearly and is dependent on the populations. By considering the age, we find that younger stars have smaller asymmetric drift, and older stars have larger asymmetric drift, which is corresponding to the velocity dispersion patterns. In the one-dimensional asymmetric drift diagram, our results confirm the previous conclusion, that is, with the increase of the vertical distance, the asymmetric drift also increases gradually, showing the “U” shape in the vertical distance diagram. The distribution of asymmetric drift in chemical space shows that high $[\alpha/\text{Fe}]$ stars have larger asymmetric drift than low $[\alpha/\text{Fe}]$ stars. Finally, we find the thick disk with a larger asymmetric drift (45 km s^{-1}). In short, we present a more complete and farther asymmetric drift map of the Milky Way disk Populations between 8–16 kpc in more details to the community.

We also notice that we are assuming in Eq. (2), a fixed rotation curve and assuming that the variations of asymmetric drift as a function of position and ages can

be derived from it. However, the rotation curve might change with Z and with the age too, so there might be a degeneracy of solutions, but so far we do not know the law very clearly about these dependence. For the moment we cannot break this degeneracy, but we only focus on the $Z = -3 \text{--} 3 \text{ kpc}$ disk region with known RC slope, as mentioned above, we just want to explore the statistical law of the asymmetric drift, the exact quantitative pattern is not expected in this current work.

With the help of different solar motions and rotation curve tests, we have also, to some extent, reduce this degeneracy influences. Moreover, this is a mainly qualitative analysis which is not touched well before, it seems that the community do not have a quite good understanding for the rotation curve-age dependences. Even for the rotation curve-Z dependence, which might be due to the asymmetric effect, so we believe that our work here is non-trivial, but more works about this project need to be done.

The non-equilibrium-state and complex dynamic perturbations of the Milky Way will produce asymmetrical drift, which is known well, and asymmetrical drift is a very important value for the dynamical history of the disturbance and the evolution of the Milky Way, which is also related to the 6D phase-space properties, radial scale length, potential, populations, etc. In the future, we will use more methods to measure asymmetric drift and consider using simulations to explore asymmetric drift to advance our understanding of the Milky Way disk solar motions, kinematics, dynamics and rotation curve.

ACKNOWLEDGEMENTS

We would like to thank the anonymous referee for his/her very helpful and insightful comments. We acknowledge the National Key R & D Program of China (Nos. 2021YFA1600401 and 2021YFA1600400). HFW acknowledges the support from the project “Complexity in self-gravitating systems” of the Enrico Fermi Research Center (Rome, Italy) and science research grants from the China Manned Space Project with NO. CMS-CSST-2021-B03, CMS-CSST-2021-A08. This is also the summer practice of the first author in 2023 with L.Y.P., who is supported by the National Natural Science Foundation of China (NSFC) under grant 12173028, the Chinese Space Station Telescope project: CMS-CSST-2021-A10, the Sichuan Science and Technology Program

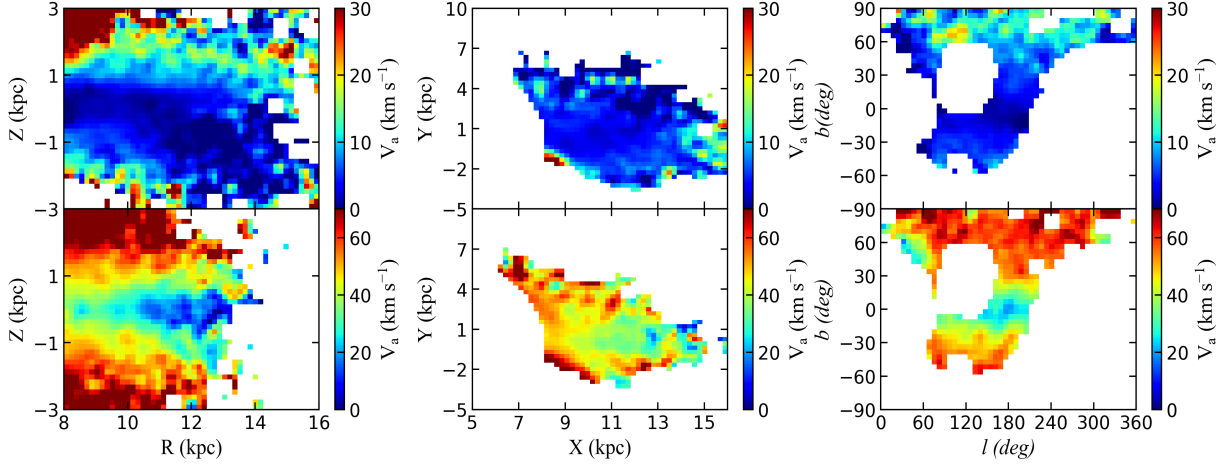


FIG. 12.— The distribution of thin and thick disk stars in the spatial coordinates. Top panel: distribution of stars in the $R-Z$, $X-Y$ and $l-b$ planes of the thin disk sample; bottom panel: distribution of the stars in the $R-Z$, $X-Y$ and $l-b$ planes of the thick disk sample.

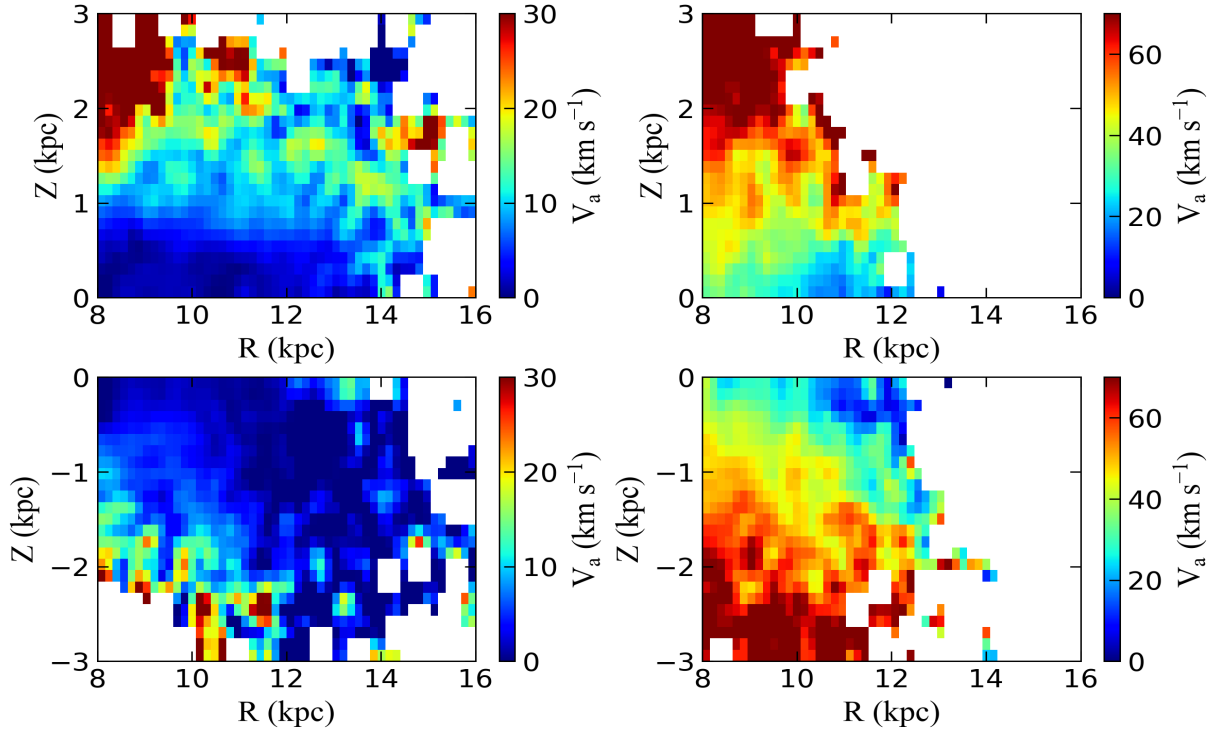


FIG. 13.— The left panel shows the distribution of the asymmetric drift of the thin disk on the north and south sides, and the right panel shows the distribution of the asymmetric drift of the thick disk on the north and south sides.

(Grant No. 2020YFSY0034), the Sichuan Youth Science and Technology Innovation Research Team (Grant No. 21CXTD0038), Major Science and Technology Project of Qinghai Province (Grant No. 2019-ZJ-A10), and the Innovation Team Funds of China West Normal University (Grant No. KCXTD2022-6).

The Guo Shou Jing Telescope (the Large Sky Area Multi-Object Fibre Spectroscopic Telescope, LAMOST) is a National Major Scientific Project built by the Chinese Academy of Sciences. Funding for the project has been provided by the National Development and

Reform Commission. LAMOST is operated and managed by National Astronomical Observatories, Chinese Academy of Sciences. This work has also made use of data from the European Space Agency (ESA) mission *Gaia* (<https://www.cosmos.esa.int/gaia>), processed by the *Gaia* Data Processing and Analysis Consortium (DPAC, <https://www.cosmos.esa.int/web/gaia/dpac/consortium>). Funding for the DPAC has been provided by national institutions, in particular the institutions participating in the *Gaia* Multilateral Agreement.

REFERENCES

Antoja, T., Helmi, A., Romero-Gómez, M., et al. 2018, *Nature*, 561, 360

Antoja, T., Ramos, P., García-Conde, B., et al. 2023, *A&A*, 673, A115

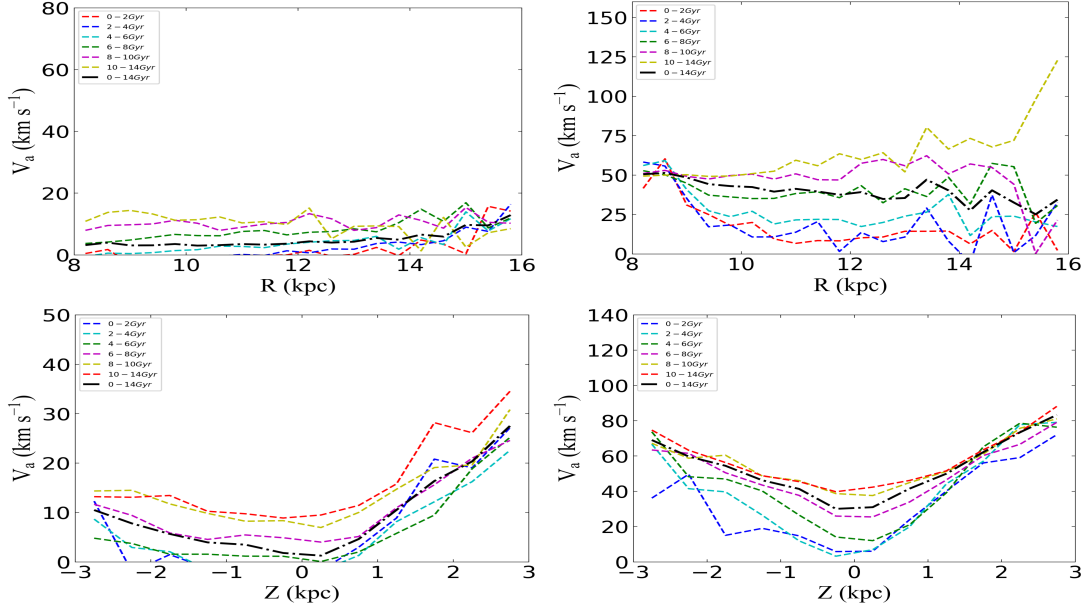


FIG. 14.— Left panels: one-dimensional distribution of the asymmetric drift of the thin disk sample along with the Galactocentric and vertical distance; Right panel: one-dimensional distribution of the asymmetric drift of the thick disk along with the Galactocentric and vertical distance.

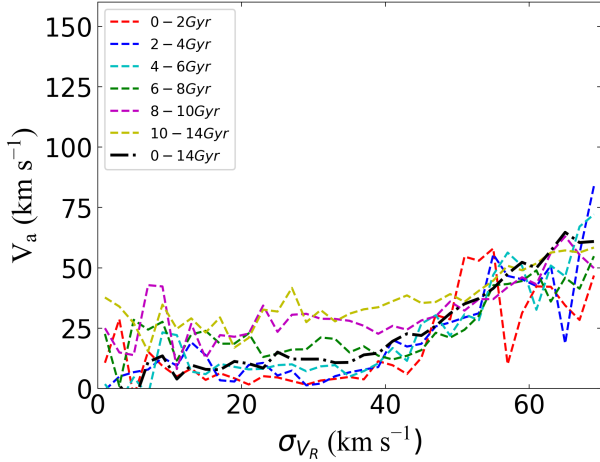


FIG. 15.— One-dimensional distribution of asymmetric drift along with the radial velocity dispersion in different stellar age populations. The black bold dotted line represents the entire sample, and other dashed lines of different colours represent stellar population of different ages.

Aumer, M. & Binney, J. J. 2009, MNRAS, 397, 1286
 Barros, D. A., Pérez-Villegas, A., Lépine, J. R. D., et al. 2020, ApJ, 888, 75
 Binney, J., & Tremaine, S. 2008, Galactic Dynamics (Princeton: Princeton University Press)
 Binney, J. 2010, MNRAS, 401, 2318
 Binney, J., Burnett, B., Kordopatis, G., et al. 2014, MNRAS, 439, 1231
 Binney, J. & Schönrich, R. 2018, MNRAS, 481, 1501.
 doi:10.1093/mnras/sty2378
 Bland-Hawthorn, J. & Gerhard, O. 2016, ARA&A, 54, 529
 Bovy, J. 2015, ApJS, 216, 29
 Carlin, J. L., DeLaunay, J., Newberg, H. J., et al. 2013, ApJ, 777, L5
 Carlin, J. L., Liu, C., Newberg, H. J., et al. 2015, AJ, 150, 4
 Chen, B., Stoughton, C., Smith, J. A., et al. 2001, ApJ, 553, 184
 Dehnen, W. & Binney, J. J. 1998, MNRAS, 298, 387
 Deng, L.-C., Newberg, H. J., Liu, C., et al. 2012, Research in Astronomy and Astrophysics, 12, 735
 Gaia Collaboration, Drimmel, R., Romero-Gomez, M., et al. 2022, arXiv:2206.06207

Eilers, A.-C., Hogg, D. W., Rix, H.-W., et al. 2019, ApJ, 871, 120
 Gaia Collaboration, Katz, D., Antoja, T., et al. 2018, A&A, 616, A11
 Gaia Collaboration, Vallenari, A., Brown, A. G. A., et al. 2022, arXiv:2208.00211
 Vieira, K., Carraro, G., Korchagin, V., et al. 2022, ApJ, 932, 28
 Golubov, O., Just, A., Bienaymé, O., et al. 2013, A&A, 557, A92
 Guiglion, G., Recio-Blanco, A., de Laverny, P., et al. 2015, A&A, 583, A91
 Kordopatis, G., Gilmore, G., Steinmetz, M., et al. 2013, AJ, 146, 134
 Hayden, M. R., Recio-Blanco, A., de Laverny, P., et al. 2018, A&A, 609, A79
 Jiao, Y., Hammer, F., Wang, H., et al. 2023, arXiv:2306.0546, A&A, in press
 Khanna, S., Sharma, S., Tepper-Garcia, T., et al. 2019, MNRAS, 489, 4962
 Kawata, D., Baba, J., Ciucă, I., et al. 2018, MNRAS, 479, L108
 Khoperskov, S. & Gerhard, O. 2022, A&A, 663, A38
 Laporte, C. F. P., Famaey, B., Monari, G., et al. 2020, A&A, 643, L3
 López-Corredoira, M., Garzón, F., Wang, H.-F., et al. 2020, A&A, 634, A66
 Li, X., Wang, H.-F., Luo, Y.-P., et al. 2023, ApJ, 943, 88
 Loebman, S. R., Roskar, R., Debattista, V. P., et al. 2011, ApJ, 737, 8
 Lee, Y. S., Beers, T. C., An, D., et al. 2011b, ApJ, 738, 187
 Mróz, P., Udalski, A., Skowron, D. M., et al. 2019, ApJ, 870, L10
 Pasetto, S., Grebel, E. K., Zwitter, T., et al. 2012, A&A, 547, A70
 Reid, M. J., Menten, K. M., Brunthaler, A., et al. 2014, ApJ, 783, 130
 Robin, A. C., Bienaymé, O., Fernández-Trincado, J. G., et al. 2017, A&A, 605, A1
 Schönrich, R., Binney, J., & Dehnen, W. 2010, MNRAS, 403, 1829
 Schönrich, R. 2012, MNRAS, 427, 274
 Siebert, A., Famaey, B., Binney, J., et al. 2012, MNRAS, 425, 2335
 Sysoliatina, K., Just, A., Golubov, O., et al. 2018, A&A, 614, A63
 Steinmetz, M., Guiglion, G., McMillan, P. J., et al. 2020, AJ, 160, 83
 Steinmetz, M., Matijević, G., Enke, H., et al. 2020, AJ, 160, 82
 Ting, Y.-S., Conroy, C., Rix, H.-W., et al. 2019, ApJ, 879, 69
 Tian, H., Liu, C., Carlin, J. L., et al. 2015, ApJ, 809, 145
 van der Kruit, P. C. & Freeman, K. C. 2011, ARA&A, 49, 301
 Wang, H.-F., López-Corredoira, M., Carlin, J. L., et al. 2018a, MNRAS, 477, 2858
 Wang, H.-F., Liu, C., Xu, Y., et al. 2018b, MNRAS, 478, 3367
 Wang, H.-F., Carlin, J. L., Huang, Y., et al. 2019, ApJ, 884, 135
 Wang, H.-F., López-Corredoira, M., Huang, Y., et al. 2020a, MNRAS, 491, 2104
 Wang, H.-F., López-Corredoira, M., Huang, Y., et al. 2020b, ApJ, 897, 119

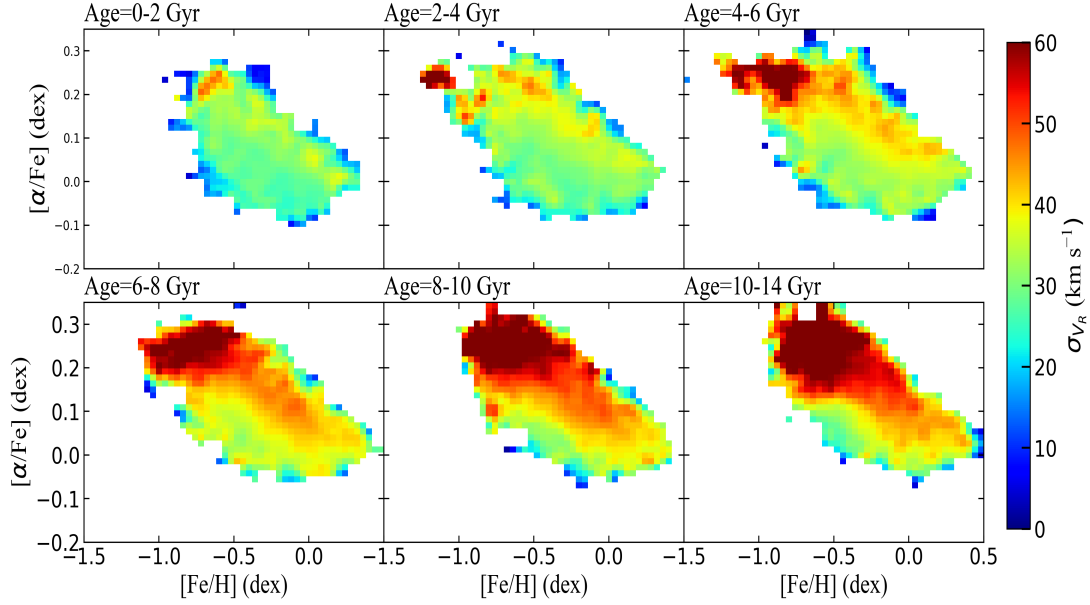


FIG. 16.— Distribution of radial velocity dispersion in the $[\text{Fe}/\text{H}]$ and $[\alpha/\text{Fe}]$ plane for different age populations.

Wang, H.-F., Huang, Y., Zhang, H.-W., et al. 2020c, *ApJ*, 902, 70
Wang, H.-F., Hammer, F., Yang, Y. B. et al. 2022, *ApJ*, 940, L3
Wang, H.-F., Chrobáková, Ž., López-Corredoira, M., Sylos Labini F., 2023a, *ApJ*, 942, 12
Wang, H.-F., Yang, Y.-B., Hammer, F., et al. 2023b, under review, eprint arXiv:2204.08542
Wojno, J., Kordopatis, G., Steinmetz, M., et al. 2016, *MNRAS*, 461, 4246
Widrow, L. M., Gardner, S., Yanny, B., et al. 2012, *ApJ*, 750, L41
Williams, M. E. K., Steinmetz, M., Binney, J., et al. 2013, *MNRAS*, 436, 101

Widrow, L. M., Barber, J., Chequers, M. H., et al. 2014, *MNRAS*, 440, 1971
Wu, Y., Xiang, M., Zhao, G., et al. 2019, *MNRAS*, 484, 5315
Xiang, M., Liu, X., Shi, J., et al. 2017, *ApJS*, 232, 2
Xiang, M., Ting, Y.-S., Rix, H.-W., et al. 2019, *ApJS*, 245, 34
Xu, Y., Liu, C., Tian, H., et al. 2020, *ApJ*, 905, 6
Yang, P., Wang, H.-F., Luo, Z.-Q., et al. 2023, *AJ*, 165, 110
Zhao, G., Zhao, Y.-H., Chu, Y.-Q., et al. 2012, *Research in Astronomy and Astrophysics*, 12, 723

This paper was built using the Open Journal of Astrophysics L^AT_EX template. The OJA is a journal which

provides fast and easy peer review for new papers in the **astro-ph** section of the arXiv, making the reviewing process simpler for authors and referees alike. Learn more at <http://astro.theoj.org>.

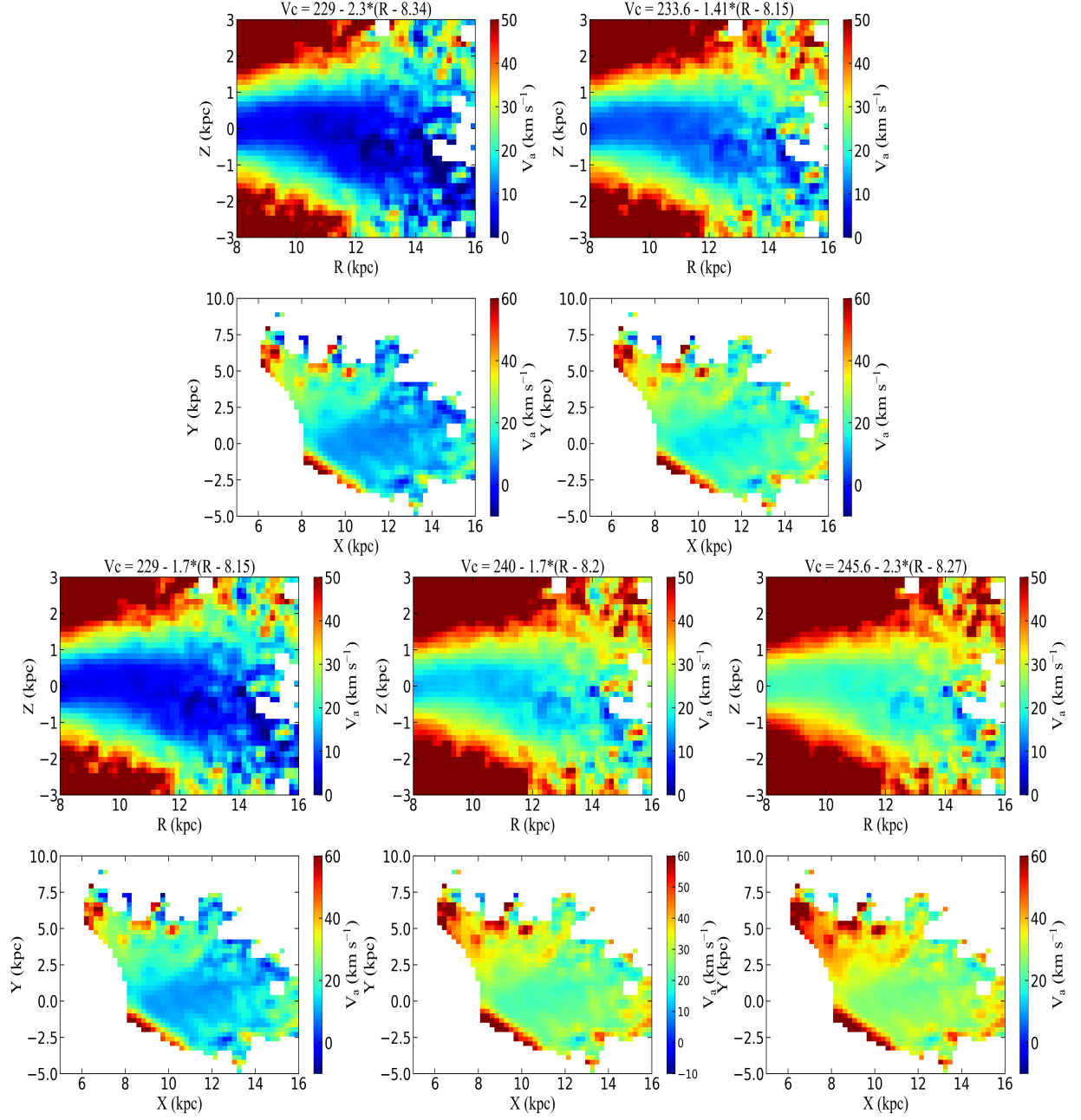


FIG. 17.— Asymmetric drift diagrams calculated from different rotation curves, Solar motions and solar location (See text at the top), these are tests considering the rotation curves differences.